Dispersion of the vapour cloud in the Buncefield Incident (pre-print)

S.E. Gant, G.T. Atkinson

Process Safety and Environmental Protection, Volume 89, Issue 6, November 2011, Pages 391-403

Dispersion of the Vapour Cloud in the Buncefield Incident

S.E. Gant[1] and G.T. Atkinson

Health & Safety Laboratory, Harpur Hill, Buxton, SK17 9JN, UK.

Tel: +44 (0)1298 218134; Fax: +44 (0)1298 218840

E-mail address: simon.gant@hsl.gov.uk

Research Highlights

- The dispersion of the vapour cloud produced in the Buncefield Incident is examined.
- Images of the visible mist from security camera records are analysed.
- CFD simulations of dense gas dispersion are presented and compared to observations.
- Cloud behaviour is shown to be affected significantly by terrain and obstacles.

Keywords

Buncefield, dense gas dispersion, CFD, terrain, obstacles

Abstract

Dispersion of the flammable vapour cloud in the 2005 Buncefield Incident is examined. Footage from security cameras around the site is analysed and the results from Computational Fluid Dynamics (CFD) simulations of the vapour dispersion are presented. It is shown that the shape of the terrain and the presence of obstacles significantly affected the dispersion of vapour from the overflowing tank. The CFD model is shown to produce similar qualitative behaviour to that observed in the incident, both in terms of the arrival time of the vapour cloud and its final depth.

[1] Corresponding author

1 Introduction

On the morning of 11 December 2005 there was a large explosion and fire at the Buncefield Oil Storage Depot near Hemel Hempstead, UK (see Figure 1). The explosion registered 2.4 on the Richter Scale, breaking windows up to 1 km away. The subsequent fire burned for several days, destroying most of the site. Over 40 people were injured and there was significant damage to commercial and residential property, but fortunately no fatalities. The cost of the incident in terms of the damage to property and loss of business is estimated to have been in the region of £1bn.

In the aftermath of the incident, the U.K. Health and Safety Executive (HSE) led a joint investigation with the Environment Agency (EA). This was overseen by the Buncefield Major Incident Investigation Board (MIIB), an independent panel of experts led by Lord Newton of Braintree. The Health and Safety Laboratory (HSL) was involved on behalf of HSE, EA and the Health Protection Agency in many scientific aspects of the investigation, including examination of damage to the site, assessment of the control and alarm systems, and analysis of the fire and explosion.

Examination of the pumping records for one of the pipelines importing fuel into the storage depot at the time of the incident indicated that there was an overfilling of one of the large tanks (Tank 912) used to store unleaded petrol shortly before the explosion (MIIB, 2006). From the time that the tank started overflowing until the explosion at 06:01, approximately 260 m^3 or 180 tonnes of petrol was released from the tank. The released liquid overflowed through vents in the roof of the tank and cascaded down the tank's sides, falling around 14 m to the bund floor. As the liquid fell, it fragmented into a spray of droplets, which partially evaporated and produced a cold, dense cloud of flammable vapour. Weather conditions were stable, humid and still at the time, and water vapour present in the air condensed in the cold vapour cloud to produce a visible mist (MIIB, 2006). Security cameras on the site recorded

images of the mist flowing in all directions away from the bund in which the overfilling tank was situated. Over a period of around 23 minutes, petrol continued to be released from the tank and the CCTV cameras recorded the mist spreading into neighbouring areas, filling the car parks of two office and manufacturing units, and eventually covering an area of approximately 500 by 400 metres across, with an average depth of around 2 m. The vapour cloud then ignited, producing a severe explosion and fire. Details of the incident investigation, including some CCTV footage of the mist and the explosion, are available on HSE's website[2].

Since the Buncefield Incident took place in 2005, there have been two large-scale incidents which have exhibited striking similarities: the Caribbean Petroleum Corporation fuel depot incident[3] in Puerto Rico on 23 October 2009, and the Indian Oil Corporation fuel depot incident[4] at Jaipur, India, on 29 October 2009. In the latter case, 12 people were killed and over 200 injured.

This paper presents one element of HSL's investigation into the Buncefield Incident, namely the use of Computational Fluid Dynamics (CFD) to study the dispersion of the flammable vapour from the overfilling storage tank. The work was undertaken to understand how the vapour cloud spread over such a large area and to provide data that could be used for explosion modelling studies. Although the simulations were performed in 2006, they have not been presented until now due to restrictions imposed by the legal proceedings. Other research undertaken by HSL into the source of flammable vapour from overfilling tank releases has been published by Atkinson et al. (2008) and Coldrick et al. (2011a; 2011b), and investigation into the explosion mechanism has been reported by the MIIB Advisory Group (2009) and by Atkinson (2011).

[2] http://www.hse.gov.uk/news/buncefield/, accessed November 2010.
[3] http://www.csb.gov/investigations/, accessed November 2010.
[4] http://oisd.nic.in/, accessed November 2010.

The first section of this paper considers the incident CCTV footage and presents maps showing the extent of the visible mist. A brief discussion is included on its likely composition: whether it was mainly water droplets (i.e. fog) or a fine suspension of petrol droplets. The second section concentrates on the CFD modelling, describing the underlying physics of the model, sensitivity tests, source conditions, and the results from dispersion simulations. Conclusions and recommendations for further work are then provided.

2 Observations from the CCTV Footage

2.1 Progress of the Mist

An aerial photograph of the Buncefield site prior to the incident is shown in Figure 2. The oil storage depot and neighbouring office buildings were equipped with more than a dozen CCTV cameras that recorded images of a visible mist shortly before the explosion. The mist first appeared flowing over the north-western edge of Hertfordshire Oil Storage Limited (HOSL) Bund A towards the water tank at approximately 05:38 (Figure 3). Shortly thereafter, the mist appeared flowing from the north-eastern edge of Bund A and across the lagoon to the north of Bund A. Five minutes after its first appearance from Bund A, it arrived in the Fuji car park and the north-eastern corner of the Northgate car park (Figure 4). It then proceeded to spread across and fill the car parks. The mist front travelling down the road to the north of HOSL Bund B was estimated at 05:43 to have an average speed of approximately 0.6 m/s. From the numerous cameras around the site, a map showing the arrival times of the mist has been produced (Figure 5).

The mist made relatively slow progress to the south from HOSL Bund A, taking more than 20 minutes to reach the top of the ramp leading up to the loading bay area. This is likely to have been due to the ground level rising in this area. To the east of the site, the mist appeared to travel relatively swiftly at first, reaching the corner of British Pipeline Agency (BPA) Bund A in 9 minutes, but then slowing down, taking another 13 minutes to travel the next 50 metres or

so further east. This may have been due to the mist passing through the hedge into the neighbouring Cherry Tree Lane. Also, this area was quite poorly lit, so the mist may have arrived here sooner, but was just not visible in the CCTV images.

2.2 Wind Speed

There were no measurements of wind speed taken on site at the time of the incident. The nearest meteorological measurements were taken at Luton airport (13 km to the east-north-east) and Northolt (24 km to the south). On the morning of the incident, these measured the weather conditions to be calm, cold, stable and humid. The wind speed was zero at Northolt, while Luton recorded an average wind speed of approximately 3 m/s from a direction of 280 degrees from north. The movement of the mist as recorded by the CCTV cameras across the Buncefield site appears to be consistent with completely zero-wind speed conditions.

2.3 Final Extent of the Mist

The final mist depths in the moments immediately before the explosion are shown on the map in Figure 6. These depths have been estimated from the relative size of neighbouring objects in the CCTV records, however, due to the variation in illumination levels across the site, the values are subject to a degree of uncertainty. Mist depths are only given to the nearest metre and the results should be interpreted accordingly. The final images taken of the Northgate and Fuji car parks were recorded around 4 minutes before the explosion. Mist depths could therefore have increased here beyond the levels shown in Figure 6.

The area immediately adjacent to HOSL Bund A and to the north, around the water tank and the lagoon, was covered with a mist around 4 metres deep moments before the explosion. Across the Northgate and Fuji car parks, the mist depth reached between 2 and 3 metres. The mist appears not to have extended to the control room at the south edge of the HOSL site, although witnesses at the tanker loading gantry reported wisps of mist being visible at their feet moments before the explosion.

The extent of the mist correlates reasonably well with the areas burnt in the subsequent explosion and fire (MIIB, 2006). The exception is the car park area to the west of the Northgate building where the mist was approximately 2 metres deep but there was no burn damage. This would suggest that the concentration of vapour here was below the Lower Explosive Limit (LEL).

2.4 What Was the Visible Mist?

When the liquid petrol cascaded from the roof of the tank, evaporation of the more volatile fractions will have lowered its temperature. Analysis of droplet evaporation indicates that vapour temperatures were probably below 0 ºC and perhaps as low as -10 ºC. A sudden drop in temperature will have caused water vapour to condense out of the air and form very small water droplets or perhaps ice crystals (essentially, fog). As the petrol vapour/mist spilled over the bund wall, it will have dispersed across the site with the visible mist appearing at the same time as the flammable vapour, the two being combined together in the gravity current.

It has been proposed by some that the visible mist could have been composed of very small petrol droplets. There are three theories as to how these formed. The first is that the vapour cloud that formed within the bund was very rich in petrol and also relatively warm, due to the liquid being released with an initial temperature of around 14 ˚C. When this warm, saturated vapour was mixed with cold fresh air, it caused some of the petrol vapour to condense and form a mist. This theory is not thought to explain correctly the mist formation for two reasons. Firstly, analysis of the CFD simulations and equilibrium calculations indicated that the temperature of the vapour produced by the evaporating petrol cascade was below 0 ˚C. Mixing fresh air at 0 ˚C with this vapour would therefore have raised rather than lowered its temperature, which should not have caused any condensation of the petrol vapour. Secondly, the addition of fresh air would have diluted the mixture and lowered the vapour pressure, making condensation less likely.

The second theory is that there was sufficiently energetic breakup of the petrol cascading from the overflowing tank to produce a significant quantity of droplets with diameter less than around 40 microns, which were subsequently carried away by the vapour flow. High-speed video footage of full-scale tank overfilling experiments (Coldrick et al., 2011a, 2011b) has shown that the mean droplet diameter at the base of the liquid cascade was probably around 2 mm. When the spray impinged on the ground, some droplets would have fragmented into smaller droplets. Based on the empirical model of Bai et al. (2002), the mean diameter of secondary particles produced by a spray impingement would be between 130 and 200 microns for dry wall impingement and between 100 and 180 microns for wet impingement. Droplets of this size would have quite rapidly fallen out of the air under the action of gravity. For the droplets to have been transported over more than 200 metres (as was observed in the CCTV footage), they must have been an order of magnitude smaller in diameter. Some size reduction could have taken place due to collisions and aerodynamic forces following the initial impingement. A further size reduction would have occurred through evaporation. To decrease the droplet diameter from 150 to 15 microns would require the mass of the droplet to decrease by a factor of 1000 (since droplet volume is proportional to the cube of its diameter). However, a decrease of the droplet mass by 99.9% seems unlikely since there was a significant fraction of heavy, relatively involatile fractions in the petrol which would have only evaporated very slowly, if at all.

The spray impingement process will have nevertheless created a fraction of droplets that were small enough to have been carried away in the vapour current. Recent work by Coldrick et al. (2011a; 2011b) has found that in full-scale overfilling tank release of hexane, the droplets appear to either fall out or evaporate completely within 10 metres of the tank. Further work is necessary to establish whether this is also the case for a multi-component liquid mixture, such as petrol. Some of the droplets in the dispersing vapour current will have been deposited as the flow passed through nearby hedges, and the lighter hydrocarbon fractions in the droplets will have continued to evaporate.

The third theory for the mist formation is that the mist was generated from the relatively warm petrol vapour, which was produced by the liquid film on the tank walls. Due to the large thermal mass of liquid in the tank, the walls would have been maintained at a temperature close to 14 ºC. Vapour produced by the petrol running down the tank walls will therefore have been warmer than that produced in the liquid cascade. As these warmer and cooler saturated vapour streams mixed, vapour will have condensed to form an aerosol. The magnitude of this effect is difficult to analyse theoretically, due to the significant uncertainties in heat and mass transfer rates, and flow recirculation in the area close to the tank wall. In the hexane tank overfilling release experiments reported by Coldrick et al. (2011a; 2011b), when the relative humidity was low, no mist was observed in the dispersing vapour current. This included conditions when the tank wall temperature was initially close to 14 ºC. However, in stable early morning conditions when the air was saturated with water vapour (dew was present on the ground), a visible mist similar in character to that observed in the Buncefield CCTV footage was produced. These experimental observations suggest that the bulk of the mist produced in the incident was condensed water vapour, not petrol droplets.

In summary, the analysis indicates that the mist observed flowing across the Buncefield site in the minutes before the explosion was composed of cold petrol vapour, made visible primarily by condensed water droplets. Within the bund surrounding Tank 912 where the petrol was being released, there will have been petrol droplets in the air due to spray breakup and splashing, and a small fraction of the droplets is likely to have persisted in the vapour current and travelled beyond the bund wall.

3 CFD Modelling of the Vapour Cloud Dispersion

3.1 Initial Model Tests

Most dense-gas dispersion models commonly used in risk assessments are unable to simulate the Buncefield incident, since it took place in nil wind. Early efforts in the Buncefield

Investigation were directed at developing a simple slumping model for the dispersion of dense gas in nil wind, similar to that presented by van Ulden (1988). However, this was unable to account for the effects of the slope and obstacles on the flow, and it soon became apparent that if these effects were ignored, the cloud dispersed too rapidly. Focus therefore shifted to developing a CFD model of the flow.

There have been a number of previous studies using CFD to predict dense gas dispersion over complex terrain (Bartzis, 1988; McBride et al., 2001; Scargiali et al., 2005). To perform CFD simulations of the vapour cloud dispersion at Buncefield across the whole area covered by the visible mist is challenging due to the relatively large flow domain and long duration of the release. In order to have good spatial and temporal resolution, the computing effort required is significant. Moreover, there are a number of uncertainties, including specifying the correct source conditions for the vapour and approximating the effects of obstructions to the vapour flow.

To address these issues, tests were first performed with a simplified CFD model of the whole site to assess the feasibility of performing detailed dispersion simulations for the full release duration. Results from this first assessment are not reported here but they showed that it was possible to run the calculations, although they would be at the limit of what could be achieved using the available computing resources at HSL at that time, with a calculation time in the order of weeks. In the second step, sensitivity studies were undertaken where each of the model uncertainties was assessed in isolation, to understand which factors were important and would require further attention, and which factors could effectively be disregarded. Rather than perform these tests using the full-scale model for the whole site, which would have taken many months, only a small region of the site was simulated. Having obtained the results from these tests, a final detailed CFD model was developed for the whole site and simulations run for the full duration of the release.

3.2 Vapour Source Term

To calculate the amount of vapour produced by the overfilling tank, the method described by Atkinson et al. (2008) was followed. This approach assumes that the spray droplets released from the tank and the surrounding vapour reach equilibrium conditions. The rate at which petrol was released from the tank was known from the pumping records. The rate at which fresh air was entrained into the overflowing tank cascade was calculated using a simple CFD simulation of a downward-directed spray with the same cross-sectional area as that observed in tank overfilling experiments. Having established the quantities of petrol and air, equilibrium calculations were performed to arrive at the source conditions, based on a simplified petrol composition, which was derived from analysis of the winter petrol that was being pumped into Tank 912 at the time of the incident, see Table 1.

The source conditions for the dispersion model were complicated by the fact that the filling rate of Tank 912 increased during the period of the release. Approximately 8 minutes before the explosion, the flow rate increased from an average of 550 m^3/hr to around 920 m^3/hr. The vapour source for the CFD model was adjusted accordingly, see Table 2.

As a check on the source term calculations, the area of ground that would be covered by a layer of vapour 2 metres deep after a 23 minute release was calculated, assuming that there was no further air entrained into the vapour cloud (see Table 2). For the 550 m^3/hr and 920 m^3/hr release rates, these areas were 257×257 m^2 and 285×285 m^2, respectively. These calculated cloud sizes are smaller than the extent of the mist visible in the CCTV records (approx. 500×400 m^2). However, some further air entrainment into the cloud would have occurred, and the depth of the visible mist was non-uniform. The vapour production rates therefore seem reasonable from this simple comparison.

The presence of condensed water droplets in the source of vapour was ignored in the CFD model. At an ambient temperature of 0 ºC, a volume of 1 m^3 of air with 100% relative humidity contains less than 5 grammes of water. Even if all of the water vapour condensed to form the visible mist, the effect on the density of the vapour current would have been negligible.

3.2 CFD Model Description

The source conditions described above were used to set the velocity, composition and temperature of the vapour that was released in the CFD model. The gas was released uniformly from the floor of HOSL Bund A in the model to produce a steady upwelling flow. This approach did not capture any large-scale unsteady motion within the bund which will have resulted from the cascades of liquid petrol produced by the overflowing tank. However, it was assumed that this would not affect the vapour cloud dispersion in the far field.

The CFD model was developed using the commercial CFD code, ANSYS-CFX version 10. To model the effect of turbulence on the mean flow, the SST model (Menter, 1994) was used with a wall treatment that switched automatically from a low-Reynolds-number approach to a turbulent wall function based on the local flow conditions and near-wall cell size. The effect of buoyancy on turbulence was accounted for using the simple gradient diffusion hypothesis with the standard CFX model constants. Since the vapour was initially 11% denser than the surrounding air, a non-Boussinesq treatment was adopted to account for density variations in the governing equations. The temperature of the ground was fixed at the ambient temperature of 0 ºC and zero-pressure entrainment boundaries were used for the top and sides of the flow domain, to allow flow to enter or escape the computational domain unimpeded.

To model the various hedges, such as those running alongside Buncefield and Cherry Tree Lanes (Figure 2), it was not feasible to use a fine grid to resolve individual trees or shrubs.

Instead, they were modelled as continuous porous regions with dimensions roughly equivalent to the hedges (details are provided below).

Second-order accurate numerical schemes were used for both the spatial and temporal discretization. The computational time-step chosen was 0.5 s, the convergence criteria was 1×10^{-4} and the maximum number of iterations per time-step was set to 5. Test simulations using a shorter time-step of 0.2 s were found to produce near-identical results. Using twice the maximum number of iterations per time-step also gave identical behaviour, and relaxing the convergence criteria by a factor of 5 produced a relatively small change in the results.

3.3 Sensitivity Tests

The sensitivity of the CFD model to various parameters was assessed using only a small region of the site, covering HOSL Bund A and the area to the west across the Northgate and Fuji car parks, as shown in Figure 7. Since the dense vapour cloud flowed along the ground and there was no wind, the domain only extended 5 metres in the vertical direction.

Tests were conducted to assess the influence of the following parameters:

- Grid resolution
- Turbulence
- Ground topology
- Hedges and obstacles
- Ground surface roughness

3.3.1 Grid Resolution

It is good practice to perform CFD simulations using a number of different computational grids with an increasingly large number of smaller cells until one obtains a grid-independent solution, where further refinement of the grid leads to no appreciable difference in the results (Casey and Wintergerste, 2000). However, a very large computational domain was required to span the Buncefield site, and it was recognized that it would be very difficult, or impossible, to achieve a fully grid-independent solution. A pragmatic approach was therefore taken where

the finest possible grid resolution was used given the available computing resources and time available, and tests were undertaken to assess the likely magnitude of errors due to possible under-resolution. A similar approach was adopted by Scargiali et al. (2005) in their simulations of dispersion of a dense vapour cloud over a 30×30 km^2 area.

The two grids used to assess the sensitivity to the grid are shown in Figure 8. To achieve the best resolution possible of the vertical span, prism-shaped cells were used for the majority of the domain. The coarse mesh used 130,000 nodes with a first cell height of 15 cm. The finer mesh used 720,000 nodes with a first cell height of 7 cm. Results from the two simulations are shown in Figure 9. The dense cloud travelled across the Northgate car park faster with the coarse grid than with the fine, a difference in the distance travelled of around 15% after 4 minutes. There were also some small differences in the stratification of the vapour cloud.

3.3.2 Turbulence

The release of liquid petrol from Tank 912 will have induced air currents and turbulence within HOSL Bund A. Characterising this turbulence level for the vapour source is extremely difficult. To examine this uncertainty, simulations were performed with two different initial turbulence levels in the source flow of vapour. The first assumed no turbulent fluctuations in the vapour source, i.e. the flow was assumed to be laminar, and the second used an inlet turbulence intensity of 10% (considered as a relatively high level for many industrial turbulent flows). The predicted maximum extent of the cloud was not significantly affected by the change in initial turbulence level in terms of the rate of cloud spread (a difference of only a few percent in distance travelled after 4 minutes), although the cloud composition was modified. In the final detailed CFD model a turbulence intensity of 5% was used.

3.3.3 Ground Topology

The effect of a slope in the ground was assessed by tilting the whole of the CFD geometry to an angle of 2.86º down towards the north, equivalent to a slope of 1:20. This does not reflect

the actual slope of the ground around HOSL Bund A, which was relatively flat. It does, however, represent a typical slope that could be encountered elsewhere on the site. The slope of the ramp leading from HOSL Bund A to the loading bay area was approximately 1:40 and the embankment between the perimeter road and Cherry Tree Lane reached 1:5 in places. Figure 10 compares results from using the 1:20 slope to those obtained using the previous flat-ground model. The difference is very significant, with the overwhelming majority of the cloud flowing directly northwards rather than west across the car parks as before. The importance of the slope of the ground was also reflected in the CCTV footage, as discussed in Section 2. These tests indicated that in the final dispersion simulations it was important to model the terrain as accurately as possible.

3.3.4 Hedges and Obstacles

The effect of hedges and obstructions on the vapour cloud flow was assessed by running simulations with and without hedges on either side of Buncefield Lane (Figure 11). The drag on the vapour flow caused by the trees and hedges was the subject of some uncertainty. CFD simulations were therefore performed using two different flow resistances that were calculated using the empirical Ergun correlation (Ergun, 1952) with volumetric porosities, ε, and characteristic length scales, L, of ε = 50 % and L =10 cm for the less porous hedge, and ε = 70 % and L = 30 cm for the more porous hedge. The results from these simulations (Figure 11) showed that the hedges clearly had a significant effect on the spreading of the vapour cloud. This was also confirmed by the CCTV footage of the incident, where the cloud depth in the Fuji car park appeared at times to be significantly deeper than in the adjoining Northgate car park, the two areas being separated by an evergreen hedge.

The Ergun correlation was used previously by Ivings et al. (2003) to model gas releases in areas congested by pipework. Having established that hedges might have a significant effect on the spreading of the vapour cloud, a more in-depth study of the literature was undertaken (Bean et al., 1975; Brandle et al., 2002; Hagen and Skidmore, 1971; Li et al., 2003; Mayhead,

1973; Wang et al., 2001; Zhou et al., 2002) which established that an alternative empirical correlation from Hoerner (1993), might be more appropriate for hedges:

$$C_2 = \frac{1}{2}\left[\frac{3}{2\varepsilon} - 1\right]^2 \quad (1)$$

where ε is the area porosity, and the flow passing through the porous region is retarded by a force proportional to the square of the flow velocity multiplied by coefficient C_2. This model was previously used by Li et al. (2003) to simulate the flow through windbreaks using CFD.

3.3.5 Ground Surface Roughness

The effect of surface roughness on the vapour cloud dispersion was assessed by performing simulations with different roughness heights of h = 0.1 mm and h = 1.0 mm, which correspond approximately to the surface of tarmac and a lawn with coarse grass, respectively. The results were found to be practically identical, and for the final dispersion model the terrain was simply treated as smooth.

3.3.6 Summary of Sensitivity Tests

In summary, the sensitivity tests showed that there were two major factors influencing the flow of vapour over the ground: the slope of the terrain and the presence of obstacles such as hedges. Turbulence levels and the grid resolution had some limited effects but predictions appeared to show that the flow was relatively insensitive to the surface roughness of the ground.

3.5 Final Dispersion Simulations

The sensitivity tests indicated that it was important to capture with as much detail as possible the slope of the terrain in order to obtain accurate predictions of the vapour cloud dispersion. To achieve this, topographical data from a photogrammetric survey commissioned by the EA was used to build the CFD model geometry. The laborious process of converting survey data to the CFD geometry introduced some localized anomalies, such as some small pits and

bumps. The general site surface levels were, however, faithfully reproduced. The contour data omitted details of the hedges, bund walls and buildings. These were added subsequently by hand, using plans and photos of the site taken prior to the incident as a guide.

A porosity of 40% was assumed for the hedge between the Northgate and Fuji car parks and the hedge in the northern half of the Fuji car park, which were composed of a dense evergreen laurel. Elsewhere, hedge porosities were assumed to be 50%. These values were taken from Bean et al. (1975) for “medium porous” shelterbelts. Two porous regions representing the resistance to the flow due to pipework and obstacles in the loading bay area and the HOSL Bund C area were also included in the model.

The top surface of the computational domain was flat and therefore the domain depth varied from approximately 5 metres in the south to a maximum of just over 10 metres in the east, where the ground level was lowest. The height of the first cell was 12 cm and in total the grid comprised 1.5 million nodes. This was the maximum resolution that could be used, given the available computing resources. A single simulation took 3 weeks, running in parallel on six 3.6 GHz and 3.8 GHz Xeon processors.

Figure 12 shows the CFD model results for the first 14 minutes of the release. The cloud shown in these plots is defined by an iso-surface at the lower explosive limit (LEL) for the petrol mixture of 1.6 % mol/mol (see Table 2). In order to compare the model results to the observations from the CCTV footage, the moment when the cloud started to flow over the bund wall has been called “time zero” ($t = 0$). The predicted progress of the cloud for the full duration of the release is also summarised in Figure 13.

The spreading rate of the vapour cloud was predicted by the CFD model (Figure 13) to be generally slightly faster than observed in the CCTV footage (Figure 5). In particular, across the Northgate car park the CFD model predicted the cloud to reach the Northgate building

after 4 minutes, whereas the CCTV footage showed it reaching there after 6 minutes. The shape of the cloud was also slightly different across the Northgate and Fuji car parks. In the CCTV footage, the cloud progressed faster across the Fuji car park than across the Northgate car park, whilst the CFD model predicted the speed to be approximately the same in the two areas.

Despite these differences, the CFD model predictions produced generally good qualitative agreement with the CCTV observations. The modelled cloud dispersed slowly in the southerly direction, similar to that observed in the CCTV footage. In the north-east of the site, although the cloud arrived slightly too early in the CFD simulations, it was predicted to flow through the hedge into Cherry Tree Lane and towards the lagoon rather than propagate further east along the north of BPA Bund A, similar to the behaviour observed in the CCTV footage. In the analysis of the CCTV footage, it was estimated that the mist travelled at around 0.6 m/s as it flowed along the road to the north of HOSL Bund B. The CFD model predicted the front speed in this area to be between 0.4 m/s and 0.6 m/s.

The predicted final depths of the vapour cloud across the site are shown in Figure 14. The height of the cloud immediately adjacent to Bund A was underpredicted by the model, mainly towards the north near the water tank where the mist level was more than 4 metres deep in the CCTV footage (see Figure 6) but only around 3 metres deep in the CFD model. However, there is generally good agreement between the CFD simulations and the observed behaviour elsewhere, particularly in the south and east. In the west, the CFD model predicted that the vapour cloud would fill the small car park area on the western side of the Northgate building to a depth of between 1 and 2 metres. Although the observed mist level in this area reached around 2 metres, the burn damage suggested that the vapour concentration was below the LEL.

A number of factors should be considered when comparing the distribution of the vapour cloud across the site in the CCTV footage and CFD model. As was mentioned earlier, estimating cloud depths from the CCTV footage was subject to some uncertainty due to the lighting level varying across the site. The CFD results shown in Figures 12 to 14 are also based on a definition of the cloud as an iso-surface at 1.6 % mol/mol petrol vapour. It is not possible to establish at what vapour concentration the mist became visible in the CCTV footage. However, results were produced with different iso-surfaces of 1 % and 2.7 % mol/mol that showed similar trends in overall behaviour.

Due to the lengthy computing time required for the CFD simulations, it was not possible to perform tests to examine the sensitivity of the results to changes in the vapour source conditions (specifically, the flow rate and density). However, the good agreement between the CFD model predictions and CCTV observations indicates that the source model of Atkinson et al. (2008) appears to provide reasonably accurate conditions. More recent analysis on the vapour source term from tank overfilling releases is presented by Coldrick et al. (2011a; 2011b).

4 Conclusions

This paper has presented an analysis of the dispersion of mist in CCTV records of the Buncefield Incident and CFD simulations of the vapour dispersion. The CCTV records showed that the mist first appeared approximately 23 minutes before the explosion. Over time, the mist layer increased in extent and in the final moments before the explosion it reached over 4 metres in depth immediately adjacent to HOSL Bund A and between 2 and 3 metres deep in the main Northgate and Fuji car park areas. The analysis showed that the visible mist comprised water droplets that had condensed from the air into the cold, dense hydrocarbon vapour, which had been produced from the overflowing tank.

The CFD simulations showed that the main factors affecting the dispersion of vapour were topography and the presence of obstacles, such as hedges. Model predictions were found to be relatively insensitive to surface roughness, whilst turbulence levels and the grid resolution had some limited effects. Results from CFD dispersion simulations for the full duration of the release showed similar qualitative behaviour to that observed in the incident, both in terms of the arrival time of the cloud and its final depth.

Whilst CFD simulations such as those presented here provide a useful tool for incident investigation, it would be challenging to apply the same methodology for the purposes of risk assessment. A range of possible release scenarios and weather conditions needs to be considered in any risk assessment, and such an analysis would not be feasible if each CFD simulation required a week or more of computing time. The Buncefield Incident took place in zero wind-speed conditions and dispersion of the dense vapour was affected strongly by topography and the presence of obstacles. Most simple dispersion models that are routinely used in risk assessment are currently unable to account fully for these effects. It would be useful in future work to investigate the feasibility of using shallow-layer models such as SPLOT (Webber and Ivings, 2004) or DISPLAY-2 (Venetsanos et al., 2003), or Lagrangian models such as QUIC (Brown et al., 2010), to address these issues.

Disclaimer

This publication and the work it describes were funded by the Health and Safety Executive (HSE). Its contents, including any opinions and/or conclusions expressed, are those of the authors alone and do not necessarily reflect HSE policy. The authors would like to thank the reviewers for their useful feedback on an earlier draft of this paper.

References

Atkinson, G., Gant, S.E., Painter, D., Shirvill, L.C., Ungut, A., 2008. Liquid dispersal and vapour production during overfilling incidents, Proc. IChemE Hazards XX Symposium & Workshop, Manchester, UK. Rugby: IChemE, p522-536, ISBN: 9780852955239.

Atkinson, G.T., 2011. Blast damage to storage tanks and steel clad buildings, Accepted for Publication, Proc. IChemE Hazards XXII Symposium & Workshop, Liverpool, UK.

Bai, C.X., Rusche, H., Gosman, A.D., 2002. Modeling of gasoline spray impingement. Atomization and Sprays 12, 1-27.

Bartzis, J.G., 1988. Flow modelling in complex terrain for atmospheric applications. Environmental Meteorology, 575-583.

Bean, A., Alperi, R.W., Federer, C.A., 1975. A method for characterizing shelterbelt porosity. Agric. Meteor. 14, 417-429.

Brandle, J.R., Zhou, X.H., Takle, E.S., 2002. The influence of three-dimensional structure of a tree shelterbelt on aerodynamic effectiveness, Land-use Management for the Future. Proc. 6th Conf. on Agroforestry in North America, Hot Springs, Arizona, USA.

Brown, M.J., Nelson, M.A., Williams, M.D., Gowardhan, A., Pardyjak, E., 2010. The Quick Urban & Industrial Complex (QUIC) chemical, biological, and radiological agent dispersion modeling system, 16th Conference on Air Pollution Meteorology, Atlanta, Georgia, USA, 17-21 January 2010

Casey, M., Wintergerste, T., 2000. ERCOFTAC Special Interest Group on "Quality and Trust in Industrial CFD" Best Practice Guidelines, version 1.0 ed. European Research Community on Flow, Turbulence and Combustion, Lausanne, Switzerland.

Coldrick, S., Atkinson, G.T., Gant, S.E., 2011a. Factors affecting vapour production in large scale evaporating liquid cascades. In Press, Process Safety and Environmental Protection.

Coldrick, S., Atkinson, G.T., Gant, S.E., 2011b. Large scale evaporating liquid cascades - an experimental and computational study, Accepted for Publication, Proc. IChemE Hazards XXII Symposium & Workshop, Liverpool, UK.

Ergun, S., 1952. Fluid flow through packed column. Chem. Eng. Prog. 48, 89-94.

Hagen, L.J., Skidmore, E.L., 1971. Windbreak drag as influenced by porosity. Trans. of the American Society of Agricultural Engineers (ASAE) 14, 464-465.

Hoerner, S.F., 1993. Fluid-Dynamic Drag. Hoerner Fluid Dynamics (publisher), ISBN 9993623938.

Ivings, M.J., Azhar, M., Carey, C., Lea, C.J., Ledin, S., Sinai, Y., Skinner, C., Stephenson, P., 2003. Outstanding Safety Questions Concerning the Use of Gas Turbines for Power Generation: Final Report on the CFD Modelling Programme of Work, HSL Report CM/03/08. Available from Health and Safety Laboratory Buxton, UK.

Li, W., Wang, F., Bell, S., 2003. Windbreak sheltering effects on an outdoor open space, Proc. 8th International IBPSA Conference, Eindhoven, Netherlands.

Mayhead, G.J., 1973. Some drag coefficients for British forest trees derived from wind tunnel studies. Agric. Meteor. 12, 123-130.

McBride, M.A., Reeves, A.B., Vanderheyden, M.D., Lea, C.J., Zhou, X.X., 2001. Use of advanced techniques to model the dispersion of chlorine in complex terrain. Trans. I. Chem. E. 79, 89-102.

Menter, F.R., 1994. Two-equation eddy-viscosity turbulence models for engineering applications. AIAA J. 32, 1598-1605.

MIIB, 2006. Buncefield Investigation Progress Report, (http://www.buncefieldinvestigation.gov.uk, accessed November 2010). Major Incident Investigation Board (MIIB).

MIIB Advisory Group, 2009. Buncefield Explosion Mechanism Phase 1, Research Report RR718. Health and Safety Executive, Sudbury: HSE Books (http://www.hse.gov.uk/research/rrpdf/rr718.pdf, accessed November 2010).

Scargiali, F., di Rienzo, E., Ciofalo, M., Grisafi, F., Brucato, A., 2005. Heavy gas dispersion modelling over a topographically complex mesoscale: a CFD based approach. Process Safety and Environmental Protection 83, 242-256.

van Ulden, A.P., 1988. The spreading and mixing of a dense cloud in still air, in: Puttock, J.S. (Ed.), Stably stratified flow and dense gas dispersion. Clarendon Press, Oxford, UK, pp. 141-168.

Venetsanos, A.G., Bartzis, J.G., Würtz, J., Papailiou, D.D., 2003. DISPLAY-2: a two-dimensional shallow layer model for dense gas dispersion inclusing complex features. J. Hazard. Mater. A99, 111-144.

Wang, H., Takle, E.S., Shen, J., 2001. Shelterbelts and windbreaks: mathematical modeling and computer simulations of turbulent flows. Ann. Rev. Fluid Mech. 33, 549-586.

Webber, D.M., Ivings, M.J., 2004. Feasibility study of modelling gas dispersion using a shallow layer approach with a robust and rigorous numerical solution technique, HSL Report CM/04/14. Available from Health and Safety Laboratory, Buxton, UK.

Zhou, X.H., Brandle, J.R., Takle, E.S., Mize, C.W., 2002. Estimation of the three-dimensional aerodynamic structure of a green ash shelterbelt. Agric. Forest Meteor. 111, 93-108.

Figure 1 Aerial photo of the Buncefield site on fire after the explosion

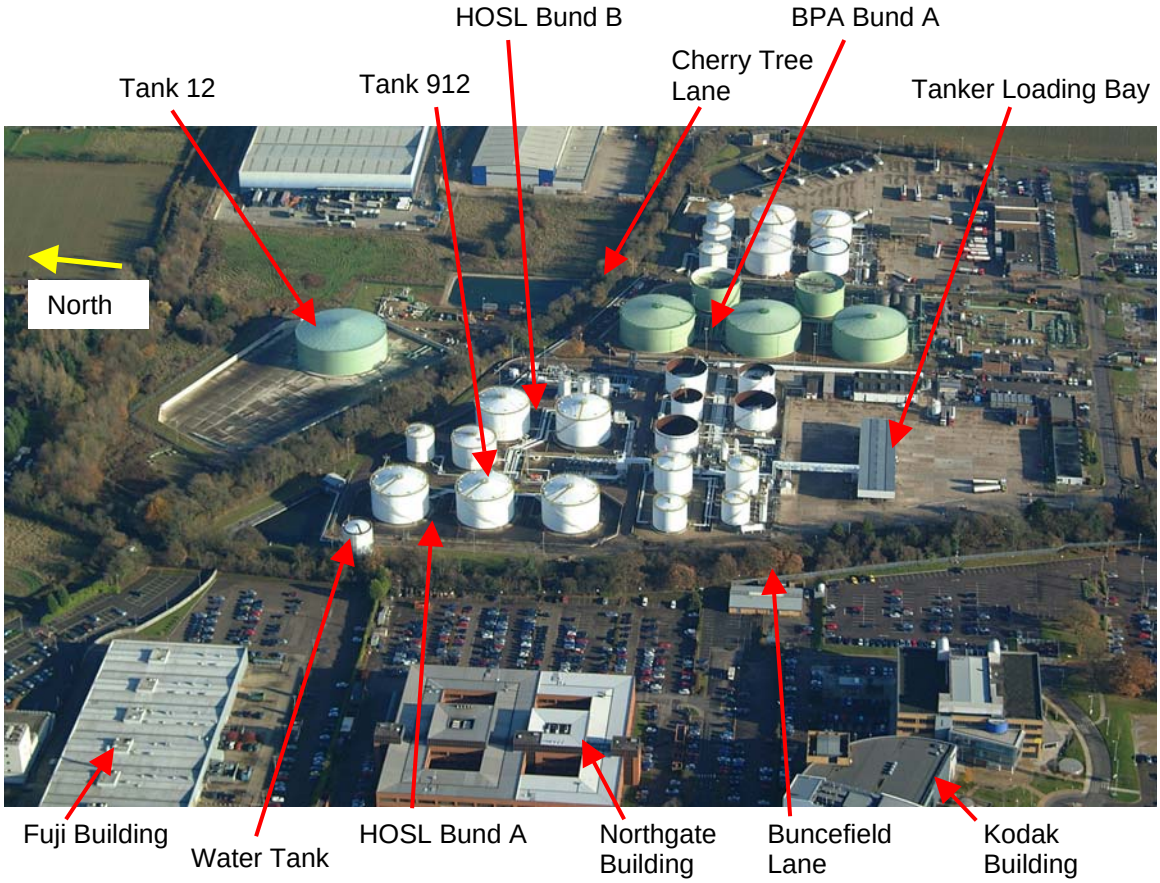

Figure 2 Aerial view looking east towards the Buncefield fuel depot and surrounding areas. The photo was taken in 2004, before the incident.

Figure 3 Images from CCTV Camera 5 looking north towards the water tank. The red lines are shown to help indicate the location of the mist front. The times shown at the top of each frame are approximately 17 minutes fast.

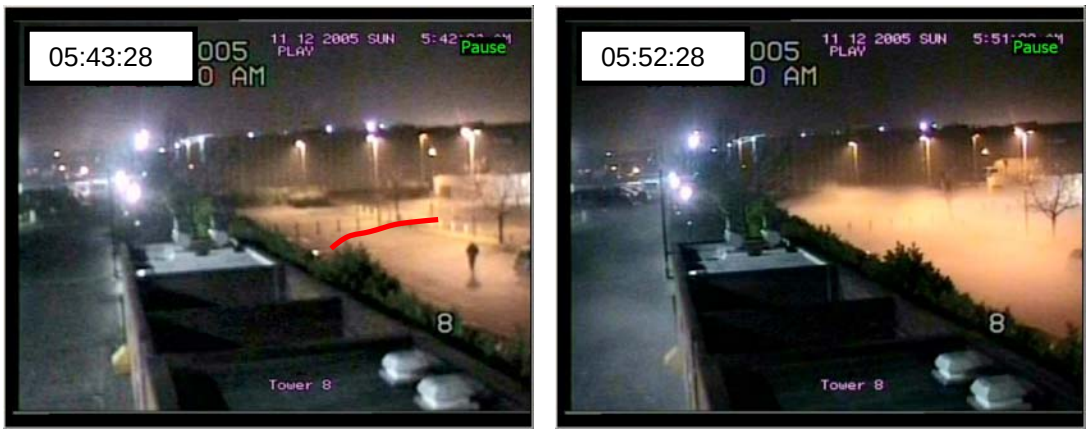

Figure 4 Images from Camera T8 looking due west showing the mist in the Fuji car park (to the right of the picture). The times shown at the top of each frame are correct.

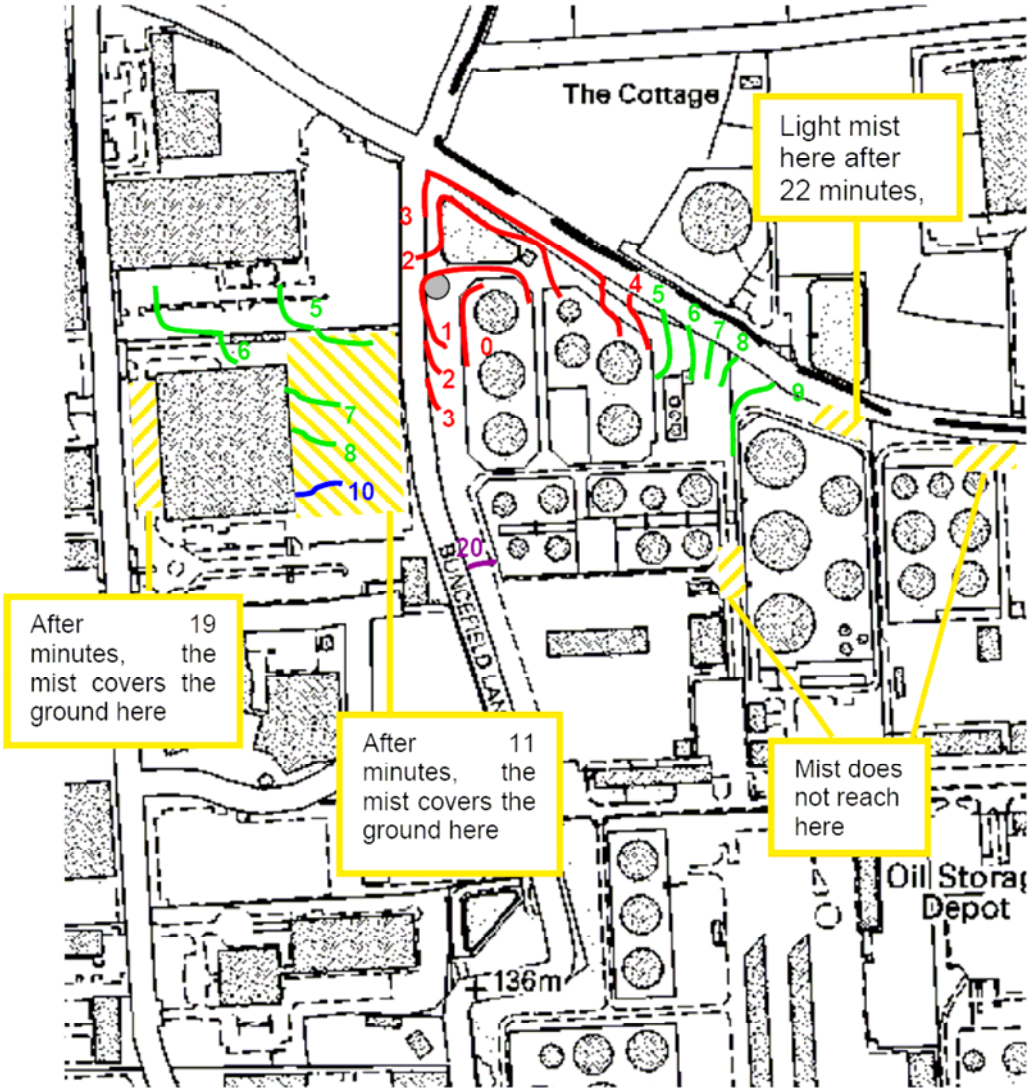

Figure 5 Approximate positions of the visible mist over time as indicated by the CCTV footage. Numbers indicate the time in minutes from the instant when the mist started to overtop the wall of HOSL Bund A. Different colours are used to help distinguish between the positions at different times.

Figure 6 Approximate final depths of the visible mist. Solid colours indicate observed depths of the mist taken directly from the CCTV cameras. Transparent colours indicate cloud heights inferred from the surrounding levels.

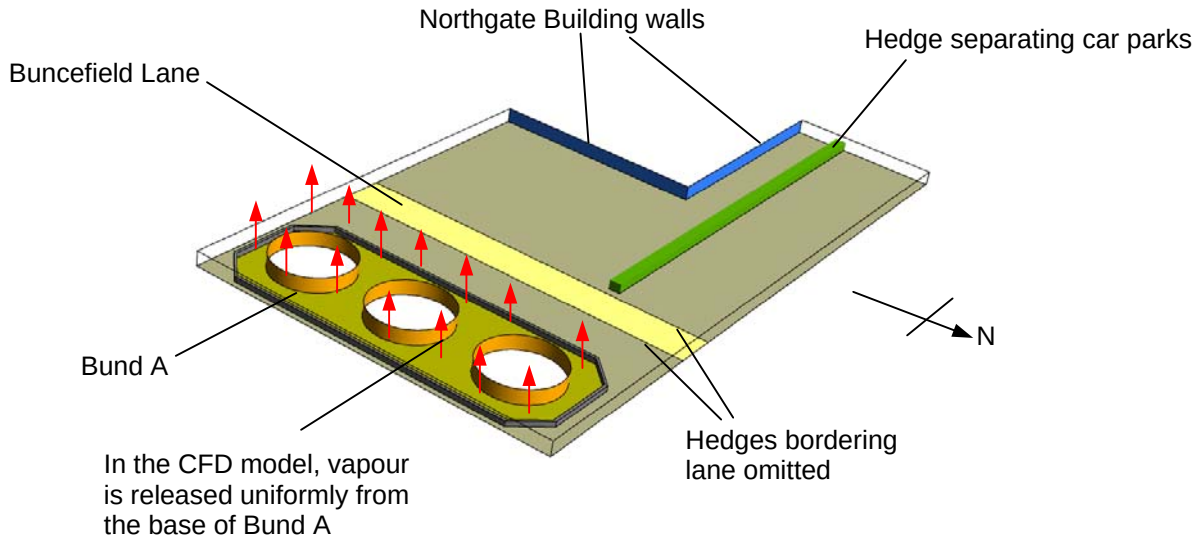

Figure 7 CFD model geometry used in the sensitivity tests.

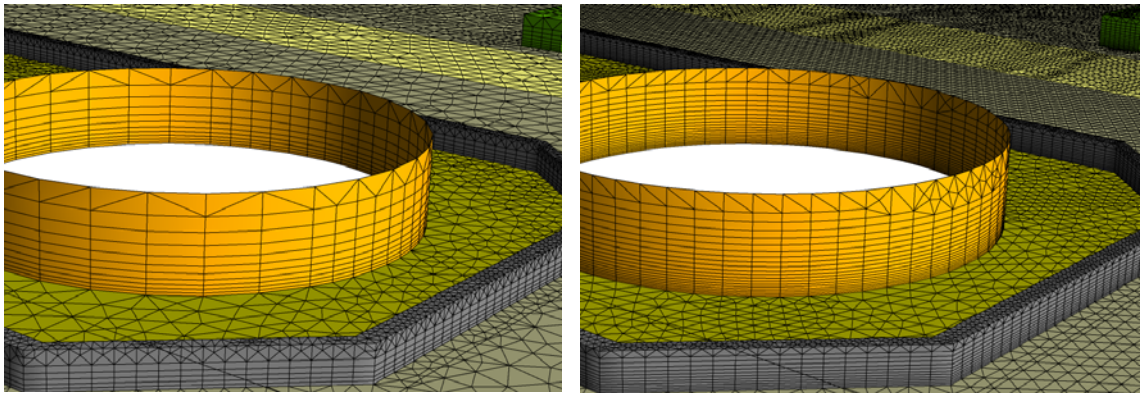

Figure 8 Close-up view of the coarse (left) and fine (right) grids used in the sensitivity tests.

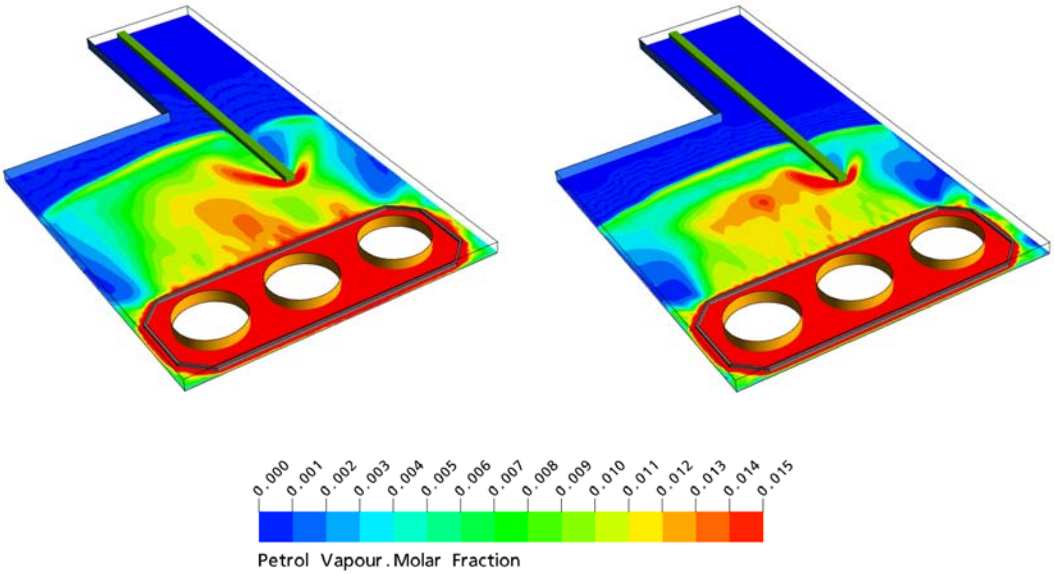

Figure 9 Petrol vapour concentrations on a plane 0.5 metres above ground level for the coarse (left) and fine (right) grids, 4 minutes after the start of the release.

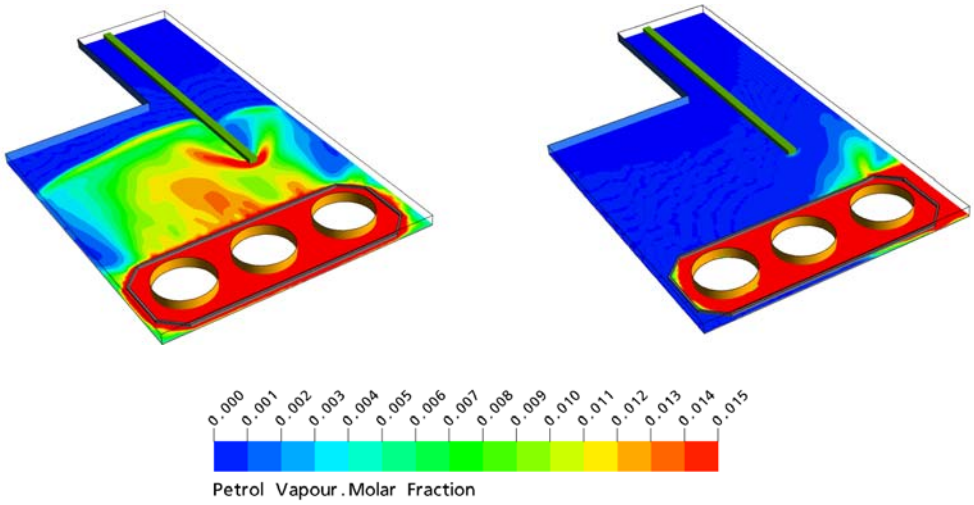

Figure 10 Petrol vapour concentrations on a plane 0.5 metres above ground level, 4 minutes after the start of the release, for completely flat ground (left) and for a 1:20 or 2.86º slope (right).

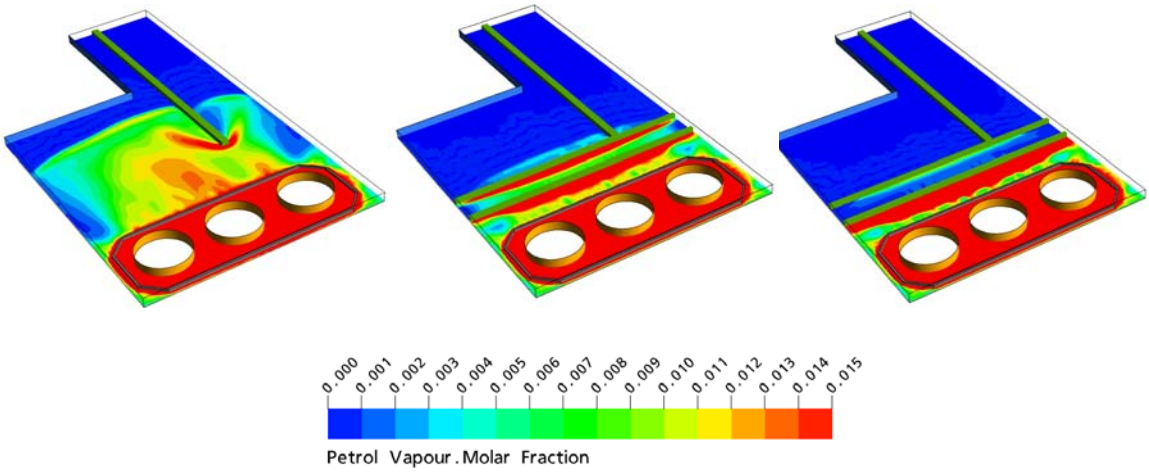

Figure 11 Petrol vapour concentrations on a plane 0.5 metres above ground level, 4 minutes after the start of the release, for an unobstructed release (left) with porous hedges alongside Buncefield lane (middle) and for less porous hedges (right).

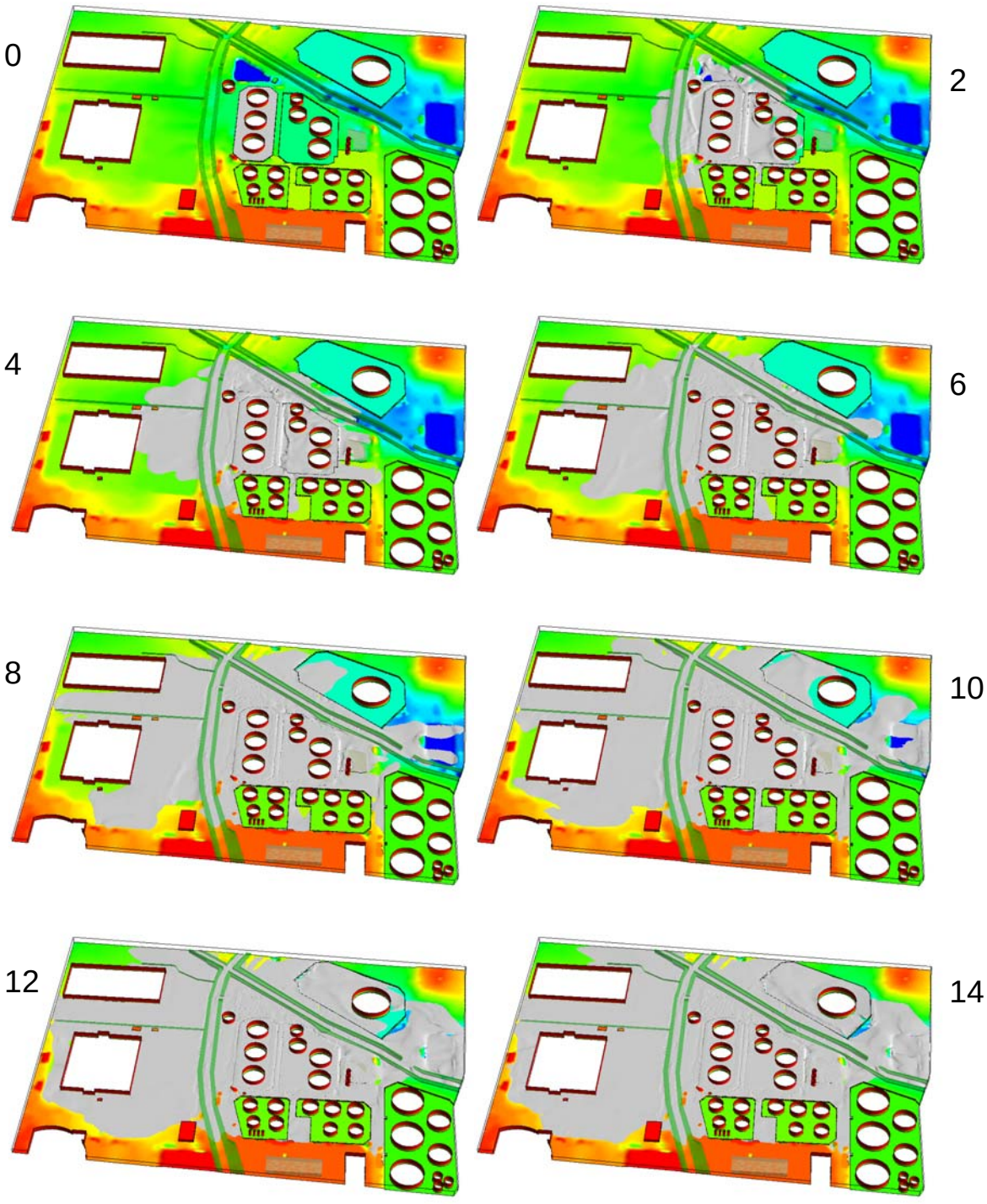

Figure 12 Dispersion of the vapour cloud over time. The ground is coloured according to elevation where dark red to dark blue represents a difference in height of 6 metres. Numbers shown indicate the time elapsed in minutes from the moment when the cloud first started flowing over the wall of HOSL Bund A.

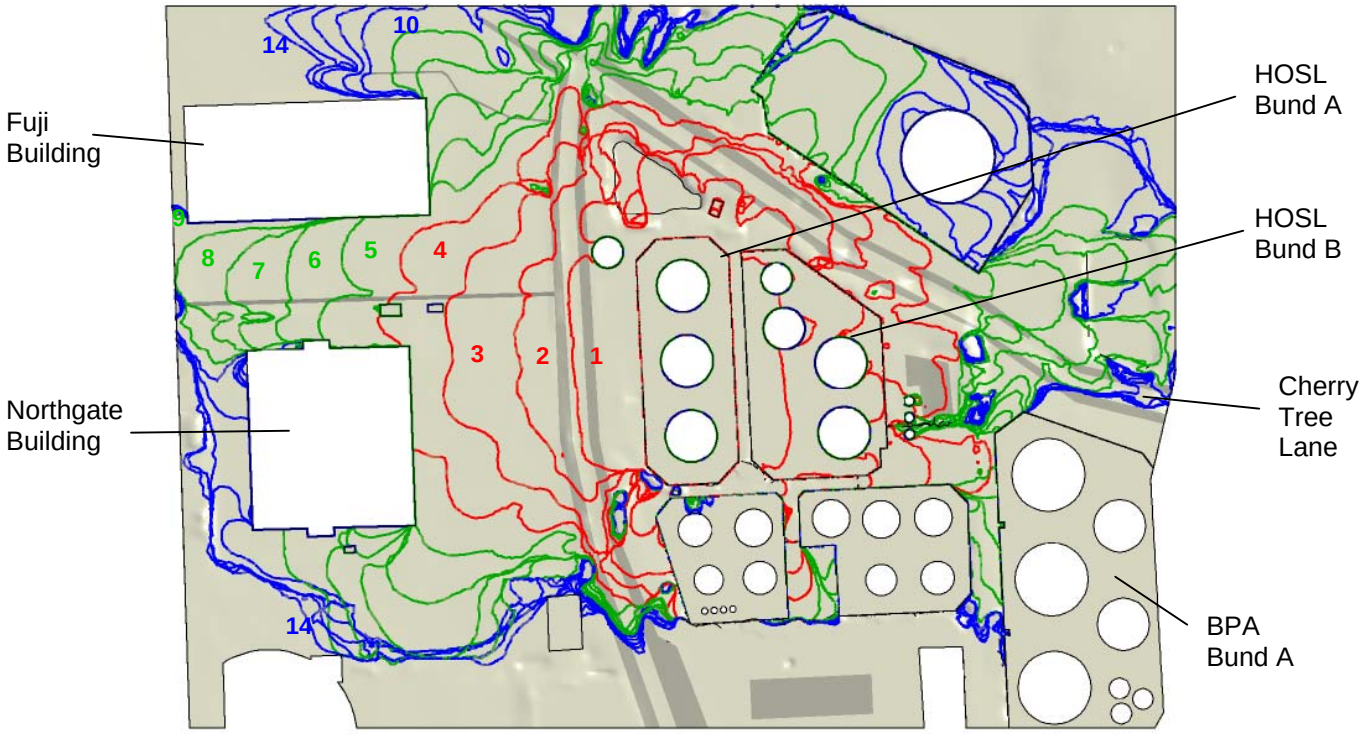

Figure 13 CFD predictions of the progress of the vapour cloud across the Buncefield site.

Times shown are in minutes from the moment the mist appeared over the wall of HOSL Bund A.

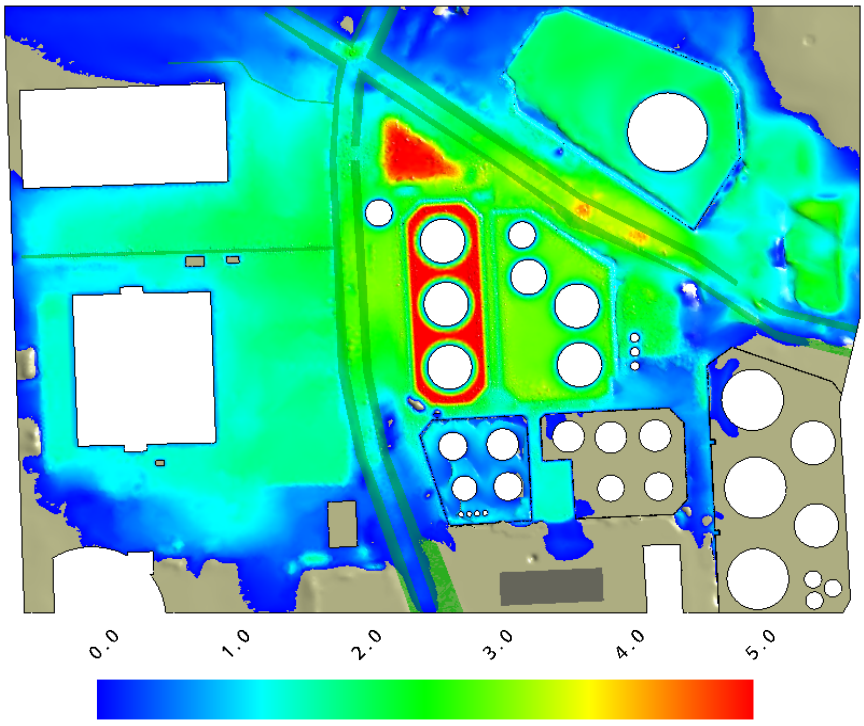

Figure 14 CFD predictions of the final vapour cloud depth (in metres)

Table 1 Summary of simplified liquid petrol composition and material properties

	Mass Fraction (% w/w)	***Relative Molecular Mass (g/mol)***	***Molar Fraction (% mol/mol)***	***Pure Liquid Density (kg/m^3)***
Butane (C_4H_{10})	9.6	58.1	16.7	585
Pentane (C_5H_{12})	*17.2*	*72.1*	24.1	631
Hexane (C_6H_{14})	16.0	86.2	18.7	665
Decane ($C_{10}H_{22}$)	57.2	142	40.6	736

Table 2 Summary of Petrol Vapour Source Conditions

Petrol Pumping Rate		***550 m^3/hr***	***920 m^3/hr***
Hydrocarbon Vapour Mass Fraction			
	Butane	5.9 % (w/w)	7.5 % (w/w)
	Pentane	6.3 % (w/w)	7.2 % (w/w)
	Hexane	2.2 % (w/w)	2.3 % (w/w)
	TOTAL	14.4 % (w/w)	17.0 % (w/w)
Hydrocarbon Vapour Molar Fraction			
	Butane	3.2 % (mol/mol)	4.2 % (mol/mol)
	Pentane	2.8 % (mol/mol)	3.2 % (mol/mol)
	Hexane	0.8 % (mol/mol)	0.9 % (mol/mol)
	TOTAL	6.8 % (mol/mol)	8.3 % (mol/mol)
Lower Explosive Limit of mixture		1.6 % (mol/mol)	1.6 % (mol/mol)
Upper Explosive Limit of mixture		8.1 % (mol/mol)	8.1 % (mol/mol)
Stoichiometric condition		2.7 % (mol/mol)	2.7 % (mol/mol)
Temperature		- 9.1 ˚C	-7.6 ˚C
Density		1.46 kg/m^3	1.47 kg/m^3
Mass Flow Rate of Air/Vapour Mixture		139 kg/s	174 kg/s
Volume Flow Rate of Air/Vapour Mixture		95.7 m^3/s	118 m^3/s
Area covered to 2m depth after 23 minutes		66,000 m^2	81,400 m^2
	(equivalent area)	(257m × 257m)	(285m × 285m)